

## Poly-*N*-methylated Amyloid $\beta$ -Peptide ( $A\beta$ ) C-Terminal Fragments Reduce $A\beta$ Toxicity in Vitro and in *Drosophila melanogaster*

Partha Pratim Bose,<sup>†,||</sup> Urmimala Chatterjee,<sup>‡,||</sup> Charlotte Nerelius,<sup>‡</sup> Thavendran Govender,<sup>†</sup> Thomas Norström,<sup>†</sup> Adolf Gogoll,<sup>†</sup> Anna Sandegren,<sup>‡</sup> Emmanuelle Göthelid,<sup>§</sup> Jan Johansson,<sup>\*,‡</sup> and Per I. Arvidsson<sup>\*,†,‡</sup>

<sup>†</sup>Department of Biochemistry and Organic Chemistry, Uppsala University, Box 576, S-75123, Uppsala, Sweden, <sup>‡</sup>Department of Anatomy, Physiology, and Biochemistry, Swedish University of Agricultural Sciences, The Biomedical Center, Box 575, S-75123, Uppsala, Sweden, and <sup>§</sup>Department of Physics and Materials Science, Uppsala University, Box 530, 751 21 Uppsala, Sweden. <sup>‡</sup>Present address: Medicinal Chemistry, Discovery CNS & Pain Control, AstraZeneca R&D Södertälje, S-151 85 Södertälje, Sweden. <sup>||</sup> Contributed equally.

Received July 22, 2009

Alzheimer's disease (AD), an age related neurodegenerative disorder, threatens to become a major health-economic problem. Assembly of 40- or 42-residue amyloid  $\beta$ -peptides ( $A\beta$ ) into neurotoxic oligo-/polymeric  $\beta$ -sheet structures is an important pathogenic feature in AD, thus, inhibition of this process has been explored to prevent or treat AD. The C-terminal part plays an important role in  $A\beta$  aggregation, but most  $A\beta$  aggregation inhibitors have targeted the central region around residues 16–23. Herein, we synthesized hexapeptides with varying extents of *N*-methylation based on residues 32–37 of  $A\beta$ , to target its C-terminal region. We measured the peptides' abilities to retard  $\beta$ -sheet and fibril formation of  $A\beta$  and to reduce  $A\beta$  neurotoxicity. A penta-*N*-methylated peptide was more efficient than peptides with 0, 2, or 3 *N*-methyl groups. This penta-*N*-methylated peptide moreover increased life span and locomotor activity in *Drosophila melanogaster* flies overexpressing human  $A\beta_{1-42}$ .

### Introduction

A key neuropathological manifestation in Alzheimer's disease (AD<sup>a</sup>) is extracellular amyloid deposits composed mainly of the 40–42 residue amyloid  $\beta$ -peptide ( $A\beta$ ).<sup>1</sup>  $A\beta$  self-assembly can generate different species in vitro.<sup>2,3</sup> Presently, there is little consensus on the relative neurotoxicity of the different species evolved from  $A\beta$  self-assembly. Mature fibrils are considered to be less important for neuronal death and impairment of hippocampal long-term potentiation than soluble intermediates, such as protofibrils, low-number oligomers, globulomers, and  $A\beta$ -derived diffusible ligands.<sup>4–6</sup> Most of the  $A\beta$  assemblies postulated to be toxic share a common feature in that they contain  $\beta$ -sheet structures. It has also been observed that fibrils can be disassembled into neurotoxic oligomers. These findings imply that therapeutic agents should target early  $A\beta$  oligomers rather than  $A\beta$  fibrils.<sup>7</sup> During the last decades, a number of strategies to prevent  $A\beta$  self-assembly and amyloid fibril formation in AD have been suggested, including inhibitors based on so-called  $\beta$ -sheet blockers.<sup>8–10</sup>

Many peptide-based inhibitors of  $A\beta$  aggregation have been reported.<sup>11</sup> Especially, short *N*-methylated peptides corresponding to parts of the central region (residues ~16–24) of  $A\beta$  have been used for designing anti-amyloid agents with attractive pharmacological properties.<sup>12–14</sup> Doig and co-workers optimized a single *N*-methyl derivative of  $A\beta$  (16–20), which prevented both aggregation and toxicity of  $A\beta_{1-42}$  toward PC12 cells in culture.<sup>15</sup>

While the central region of  $A\beta$  has attracted much attention, the role of the C-terminal region has been far less explored despite the facts that this region forms intermolecular  $\beta$ -sheet contacts in  $A\beta$  fibrils and was previously proposed to be the kinetic determinant of the self-assembly process.<sup>16</sup> More recently, it was also demonstrated that peptides derived from  $A\beta$  positions 28–42 were efficient in protecting neurons from  $A\beta$  toxicity, again pointing to the importance of the C-terminal region.<sup>17</sup>

As we recently reported the first high-resolution structure of a poly-*N*-methylated peptide<sup>18</sup> and observed that peptides containing consecutive *N*-methyl amino acids have a high propensity of adopting an extended  $\beta$ -strand conformation, we became interested in evaluating if peptides with multiple *N*-methylated amide bonds also were capable of inhibiting protein aggregation caused by intermolecular  $\beta$ -sheet formation. Thus, we hypothesized that *N*-methylated peptides derived from the C-terminal sequence of  $A\beta$  could act as inhibitors of  $A\beta$  self-assembly mainly for two reasons. First, their conformational preference for adopting a  $\beta$ -strand structure should allow interference with the archetypal amyloid intermolecular  $\beta$ -sheet aggregation and thus disrupt the process of self-assembly. Second, sequence specificity should allow modulation of the parallel in-register interactions

\*To whom correspondence should be addressed. For P.I.A.: phone, +46-8-55325923; fax, +46 18 4713818; E-mail, Per.Arvidsson@biorg.uu.se. For J.J.: phone, +46-18-7414065; fax, +46-18-550762; E-mail, Jan.Johansson@afb.slu.se.

<sup>a</sup> Abbreviations: AD, Alzheimer's disease;  $A\beta$ , amyloid  $\beta$ -peptides; AFM, atomic force microscopy; BTC, bis(trichloromethyl)carbonate; CD, circular dichroism; DIPEA, diisopropyl ethyl amine; ELSD, evaporative light-scattering detection; Fmoc, 9-fluorenylmethoxycarbonyl; HATU, *O*-(7-azabenzotriazole-1-yl)-*N,N,N',N'*-tetramethyluronium hexafluorophosphate; HFIP, 1,1,1,3,3,3-hexafluoroisopropanol; Mep-*tides*, *N*-methylated peptides; MTT, 3-(4, 5-dimethyl thiazol-2-yl)-2,5-diphenyltetrazolium bromide; TBTU, *O*-(benzotriazol-1-yl)-*N,N,N',N'*-tetramethyluronium tetrafluoroborate; TEM, transmission electron microscopy; PBS, phosphate buffered saline

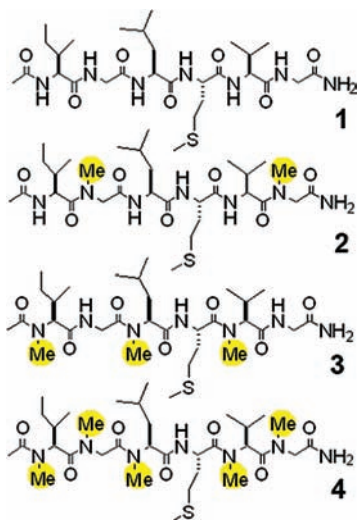


**Figure 1.** Structures of the *N*-methylated peptides 1–4.

underlying  $A\beta$  self-assembly.<sup>1</sup> Herein, we report our findings of a novel poly-*N*-methylated peptide derived from the  $A\beta$  C-terminal region capable of decreasing  $A\beta$   $\beta$ -sheet and fibril formation and neurotoxicity in vitro and in vivo.

## Results

**Design and Synthesis of Poly-*N*-methylated Peptides.**  $A\beta$  is amphiphilic because of its first 28 residues being mainly polar (including 12 charged residues at neutral pH) and the last 12 (for  $A\beta_{1-40}$ ) or 14 (in  $A\beta_{1-42}$ ) residues being mainly non-polar.  $A\beta$  aggregates and forms higher-order oligomers in vitro, but the molecular pathway(s) underlying generation of soluble oligomers, insoluble fibrils, and other neurotoxic species are not entirely known.<sup>1,19</sup> Intermolecular interactions involving  $A\beta$  C-terminal region has been proposed in relation to generation of neurotoxic  $A\beta$  oligomers.<sup>20–22</sup> Urbanc et al. showed the formation of a crucial turn structure centered at Gly(37)–Gly(38) and stabilized by an intramolecular contact between Val(36)–Val(39), which is a key structural formation in  $A\beta$  monomer which effectively paves the way for the generation of pentameric nucleus for  $A\beta$  (particularly for  $A\beta_{1-42}$ ).<sup>21</sup> Met(35), and the side chains of neighboring residues, in the full length  $A\beta$  sequence has also been suggested to play a role in paranucleus formation.<sup>21,23</sup> Recently, it has been found that C-terminal fragments (covering residues 31–42 or parts thereof) may be incorporated into the putative hydrophobic core of  $A\beta_{1-42}$  oligomers consequently disrupting the same, thereby reducing  $A\beta_{1-42}$  toxicity.<sup>17</sup> Hence, Met(35) and its neighboring residues are apparently important for early  $A\beta$  self-assembly. With this in mind, we focused our efforts on analogues of the C-terminal end of  $A\beta$ , i.e., position 32–37. Thus Meptide 1–Meptide 4 (1–4), containing 0, 2, 3, or 5 methyl groups, respectively (Figure 1), were designed and synthesized.

Peptides were synthesized using solid-phase peptide synthesis employing the Fmoc-protecting group strategy. The nonmethylated peptide 1 was synthesized using a Pioneer Applied Biosystems synthesizer. For coupling, TBTU in combination with DIPEA was used. The resin used for the parent peptide contained the Rink amide linker in order to produce the C-terminal amide. Standard procedures, 95:2.5:2.5 (TFA, TIS, H<sub>2</sub>O), were used for cleavage of the peptide from the resin and removal of side-chain protecting

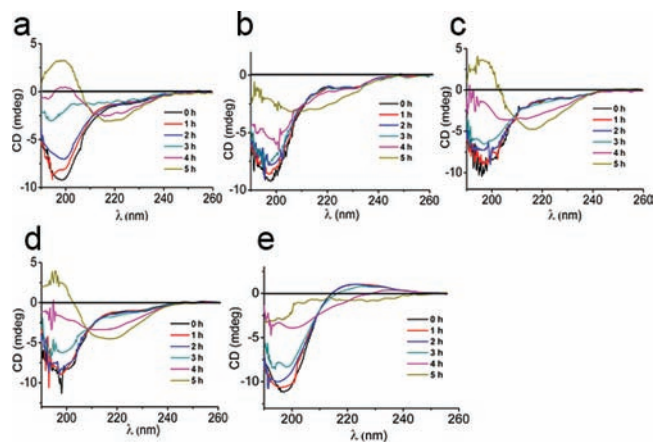


**Figure 2.** CD spectra for 20  $\mu\text{M}$   $A\beta_{1-40}$  over 5 h (a) alone or in the presence of 100  $\mu\text{M}$  of (b) 1, (c) 2, (d) 3, (e) 4.  $A\beta$  was incubated either alone in 10 mM sodium phosphate buffer, pH 7.4, at 37 °C under agitation, or in the presence of 100  $\mu\text{M}$  1–4.

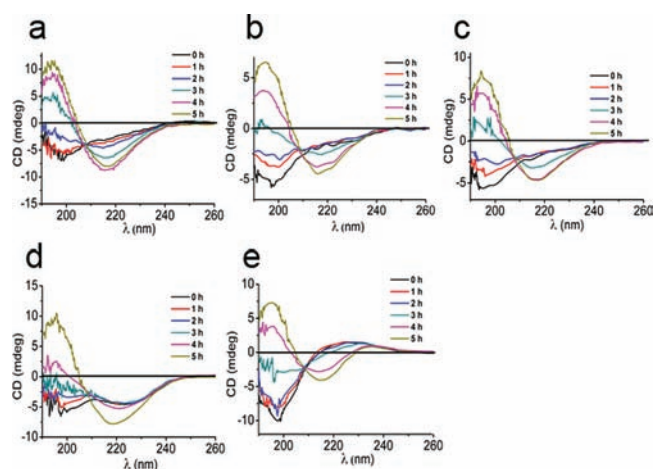


**Figure 3.** CD spectra for 20  $\mu\text{M}$   $A\beta_{1-42}$  over 5 h (a) alone or in the presence of 100  $\mu\text{M}$  of (b) 1, (c) 2, (d) 3, (e) 4.  $A\beta$  was incubated either alone in 10 mM sodium phosphate buffer, pH 7.4, at 37 °C under agitation, or in the presence of 100  $\mu\text{M}$  1–4.

groups. The known challenges associated with the synthesis of peptides containing consecutive *N*-methyl amino acids<sup>24,25</sup> forced us to employ special techniques for the preparation of 2–4. The syntheses were performed by manual solid phase peptide synthesis on a Sieber resin with HATU as coupling reagent. The high acid sensitivity of this linker allowed the highly acid sensitive poly-*N*-methyl peptide 4 to be cleaved by mild acidic conditions (2% TFA in DCM). Full synthetic details are given in the Experimental Procedures and Supporting Information. All Fmoc-*N*-methyl amino acids were synthesized according to a procedure previously reported by us.<sup>18,26</sup>

**Effects on  $A\beta$   $\beta$ -Sheet Formation by 1–4.** Conformational homogeneity of  $A\beta$  samples is a prerequisite for reproducibly monitoring  $A\beta$  self-assembly. We have adopted a protocol that employs pretreatment with trifluoroacetic acid and hexafluoroisopropanol with some modifications, as described in the Experimental Procedures.<sup>27,28</sup> Circular dichroism (CD) experiment confirmed that this results in  $A\beta$  samples with mainly unordered structure; see Figures 2a and 3a.

CD spectroscopy is suitable for monitoring folding and aggregation kinetics.<sup>27,29,30</sup> A common picture emerging

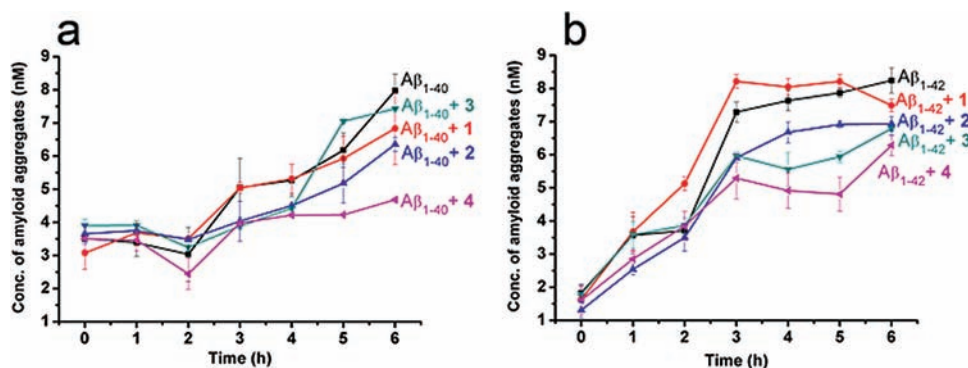


**Figure 4.** Effects of **1–4** on Congo red binding of (a)  $A\beta_{1-40}$  and (b)  $A\beta_{1-42}$ .  $A\beta$ s (20  $\mu$ M) were incubated with or without **1–4** (100  $\mu$ M) in 10 mM sodium phosphate buffer, pH 7.4, at 37  $^{\circ}$ C under agitation. Error bars represent standard deviation ( $n = 3$ ).

from biophysical studies suggests that  $A\beta$  exists in a “natively unfolded” conformation and undergoes nucleation-dependent self-assembly. It is suggested that  $A\beta$  can form pentameric or hexameric “paranuclear” units, which self-associate to form beaded protofibrils, which further aggregate to form fibrils, ultimately leading to plaque formation.<sup>1</sup> Throughout this self-assembly process,  $\beta$ -sheet structures become more and more prominent.<sup>31</sup>

To evaluate the effects of **1–4** on  $A\beta$  aggregation, we therefore used CD spectroscopy to monitor formation of  $\beta$ -sheet structure, from a predominantly unordered initial state, during early assembly stages (0–5 h). The C-terminal part of  $A\beta_{1-42}$  is more rigid than that of the more abundant and less toxic  $A\beta_{1-40}$ .<sup>32–34</sup> This higher conformational stability of C-terminal  $A\beta_{1-42}$  apparently makes it more prone to aggregation and allows the formation of oligomer populations with higher neurotoxicity than  $A\beta_{1-40}$ .<sup>19–22</sup> We therefore evaluated the potential of **1–4** against both  $A\beta_{1-40}$  and  $A\beta_{1-42}$ , using a 5-fold molar excess of ligands. CD spectroscopy showed that changes in secondary structure indeed differ between  $A\beta_{1-40}$  and  $A\beta_{1-42}$  during the first 5 h (Figures 2a and 3a). Inhibitor spectra were subtracted from the corresponding spectra of inhibitor treated- $A\beta$ . The CD spectra of inhibitors are shown in Supporting Information Figure S1. The inhibitors themselves did not show any change in CD spectra within the experimental time course (5 h).

The first CD sign of conversion from unordered to  $\beta$ -sheet structure (loss of minimum around 200 nm and occurrence of a broad minimum around 217 nm) occurred after 2 h for  $A\beta_{1-42}$  but first after 4 h for  $A\beta_{1-40}$  (Figures 2a and 3a). Moreover, **1–4** had different effects on the first occurrence of  $A\beta_{1-40}$  and  $A\beta_{1-42}$   $\beta$ -sheet structure. The nonmethylated **1** and the di- or trimethylated **2** and **3** retarded the appearance of  $\beta$ -structure for  $A\beta_{1-40}$  to 4–5 h (Figure 2b–d) and for  $A\beta_{1-42}$  to 3 h (Figure 3b–d). The penta-methylated **4**, in contrast, completely prevented  $\beta$ -sheet formation of  $A\beta_{1-40}$  during the time period studied (Figure 2e) and delayed the appearance of  $A\beta_{1-42}$   $\beta$ -sheet structure to 4 h (Figure 3e). This suggested that **4** is more efficient than the less methylated peptides in reducing formation of soluble oligomers with  $\beta$ -sheet structure from  $A\beta_{1-40}$  and  $A\beta_{1-42}$ . We tested the efficiency of **3** and **4** against  $A\beta_{1-40}$  using a 1:1 molar ratio between  $A\beta$  and ligand. Ligand **3** showed no effect on the CD spectra of  $A\beta_{1-40}$  over a 5 h period, while **4** prolonged the appearance of  $\beta$ -sheet structure until 4 h (data not shown). Monitoring, the residual molar ellipticity at 217 nm over time likewise shows different effects of **1–4** on

the evolution of  $A\beta_{1-40}$  and  $A\beta_{1-42}$   $\beta$ -structure (Supporting Information Figure S2). Moreover, deconvolution of CD spectra using SELCON3 algorithm support these conclusions.<sup>35,36</sup> The  $\beta$ -structure content of  $A\beta_{1-40}$  at time 0 was  $\sim$ 25%, in accordance with the recent data,<sup>37</sup> and increased to about 45% at 5 h. The content of unordered structure at time 0 was about 42%, which decreased to  $\sim$ 25% after 5 h. In the presence of **1**, **3**, and **4**, the  $A\beta_{1-40}$   $\beta$ -structure contents at 5 h were 25–30%. Notably, in the presence of **4**, the content of unordered structure was increased to about 55% after 5 h. This supports a stabilization of  $A\beta_{1-40}$  monomers by in particular **4** within the experimental time course. For  $A\beta_{1-42}$ , deconvolution of CD spectra with and without inhibitors showed that in the presence of **4**, there was a significant increase in unordered structure already at time 0 (about 30% in native  $A\beta_{1-42}$  and about 50% in the presence of **4**).

To further assess whether **1–4** were able to reduce formation of amyloid-like aggregates, Congo red binding assay was used.<sup>38</sup> As seen in Figure 4, **4** reduced the formation of Congo red positive assemblies from  $A\beta_{1-40}$  and  $A\beta_{1-42}$  in line with its ability to reduce the formation of  $\beta$ -sheet structure. On the other hand, **1–3** could not reduce the formation of Congo red positive aggregates as effectively as **4** (Figure 4a,b). These results together suggest that **4** has promising inhibitory effect on the aggregation of  $A\beta$ .

**Effects on Abundance and Morphology of  $A\beta$  Fibrils by **1–4**.** Transmission electron microscopy (TEM) can be used to assess the impact of inhibitors on  $A\beta$  fibril’s overall abundance and morphology.<sup>39</sup> The effects of **1–4** on formation of  $A\beta_{1-40}$  amyloid fibrils were studied for a minimum of two separate samples prepared at different occasions. The whole EM grid was examined and a minimum of eight different representative fields were used for classification of fibril density and morphology. As for effects on formation of  $\beta$ -sheet structure and Congo red positive aggregates, the peptide’s efficacy to reduce the number of fibrils increased with increasing degree of *N*-methylation. Peptide **4** inhibited fibril formation of  $A\beta_{1-40}$  to a large extent and the fibrils obtained after coincubation with **4** were shorter, while **3** was less efficient. Peptides **1–2** had little or no effects (Figure 5, and Supporting Information Table 2). Oxidizing the methionine side-chain of **4** (**4Ox**, Supporting Information Figure S3b) to the more hydrophilic sulfone reduced the inhibitory capacity with no observable effect on the occurrence or length of fibrils (Supporting Information Figure S4b and Table 2). As a control, a peptide consisting of five *N*-methylated alanine residues, (NMe-Ala)<sub>5</sub> (Supporting Information

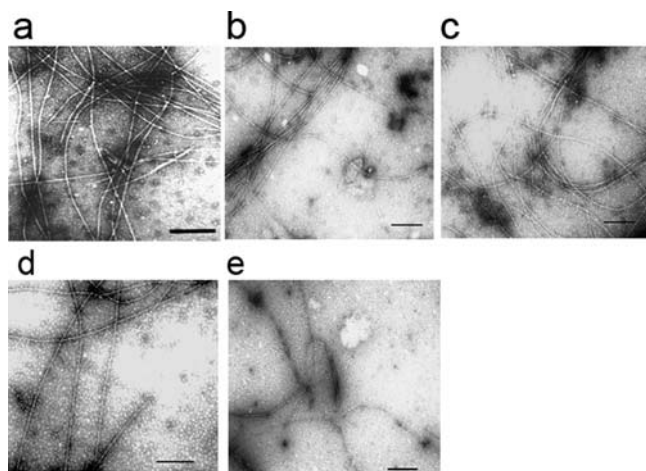


**Figure 5.** Transmission electron microscopy of (a) 25  $\mu\text{M}$   $A\beta_{1-40}$  alone or in the presence of 125  $\mu\text{M}$  (b) **1**, (c) **2**, (d) **3**, (e) **4**. The scale bars measure 100 nm. All samples were incubated in 10 mM sodium phosphate buffer, pH 7.4, at 37 °C for 72 h.

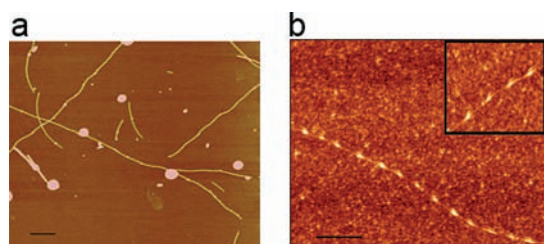


**Figure 6.** AFM in tapping mode of fibrils formed from (a) 20  $\mu\text{M}$   $A\beta_{1-40}$  alone or (b) in the presence of 100  $\mu\text{M}$  **4** after incubation for 5 days in 10 mM sodium phosphate buffer, pH 7.4, at 37 °C under agitation. The scale bars measure 500 nm. Inset in b shows a close-up to emphasize the altered fibril morphology.

Figure S3a) was used and showed to have no effect on  $A\beta_{1-40}$  fibril formation (Supporting Information Figure S4a and Table 2). The results with **4Ox** and **(NMe-Ala)<sub>5</sub>** indicate sequence specificity of the inhibitors.

Atomic force microscopy (AFM) can provide further insights into the  $A\beta$  morphology, and it can be used to explore factors that affect fibril formation. Moreover, AFM is label-free and provides high resolution structural details.<sup>40,41</sup> Because CD, Congo red, and TEM experiments suggested that **4** is the most potent of the peptides now studied, we used ex situ AFM to explore the impact of **4** on fibril formation of  $A\beta_{1-40}$  in more detail. This showed the morphology of the fibrils formed in the presence of **4** was different, and the number of fibrils was dramatically lowered, as compared to the sample of  $A\beta_{1-40}$  alone (Figure 6 and Supporting Information Figure S5). Indeed, as seen in Figure 6, fibrils formed in the presence of **4** appeared as “beads on a string” with a definite periodicity. Each of the repeat units had very similar dimensions. Another striking difference between **4** treated  $A\beta_{1-40}$ , as compared to untreated  $A\beta$  fibrils was the absence of globular aggregates (Figure 6). To conclude, **4** altered both the morphology and reduced the abundance of  $A\beta$  fibrils.

**Effect of  $A\beta_{1-42}$  Toxicity on PC12 Cells.**  $A\beta$  self-assembly generates assemblies that are toxic to cells in culture. The ability of the meptides (**1–4**) to reduce  $A\beta$  aggregation indicated that they may be useful in protecting cells from  $A\beta$  induced toxicity. For this purpose an

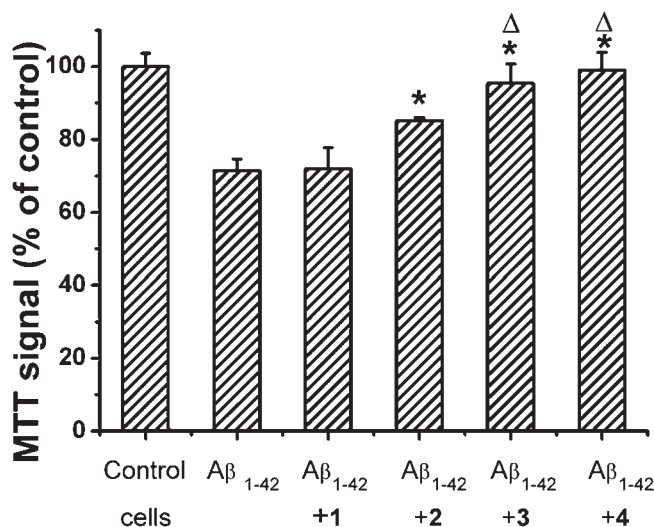


**Figure 7.** Effects of **1–4** on  $A\beta_{1-42}$  toxicity to PC12 cells. Cells were treated with  $A\beta_{1-42}$  (2  $\mu\text{M}$ ) alone or  $A\beta_{1-42}$  plus **1–4** (10  $\mu\text{M}$ ) for 4 h after which ability to reduce MTT was measured. Error bars represent standard deviation ( $n=3$ ). \* >  $A\beta_{1-42}$  alone and  $A\beta_{1-42}$  + **1** ( $p < 0.001$ ),  $\Delta$  >  $A\beta_{1-42}$  + **2** ( $p < 0.001$ ) as analyzed by Student's  $t$  test. One representative experiment out of three is shown.

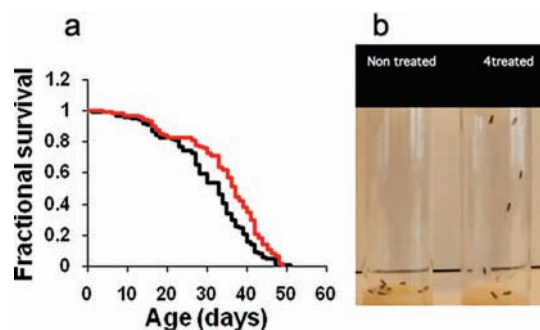


**Figure 8.** (a) Meptide **4** prolongs lifespan of  $A\beta_{1-42}$  transgenic flies. Kaplan–Meier plots of nontreated  $A\beta_{1-42}$  *Drosophila melanogaster* flies kept at 29 °C (black, median survival 30 days,  $n=98$ ) and  $A\beta_{1-42}$  flies treated with 300  $\mu\text{M}$  **4** (red, median survival 34 days,  $n=100$ ).  $P$  Value for nontreated vs **4** treated equals 0.004. (b) Frame from the video of locomotor activity assay with **4** treated and non treated transgenic  $A\beta_{1-42}$  *Drosophila melanogaster* flies. (See Supporting Information for full movie video).

MTT (3-(4, 5-dimethylthiazol-2-yl)-2–5 diphenyltetrazolium bromide) assay was employed to monitor oxidative capacity of PC12 cells<sup>42,43</sup> after treatment with  $A\beta_{1-42}$  polymerized in the absence or presence of **1–4**. Again, efficiency correlated with the number of  $N$ -methyl groups (Figure 7). Peptide **1** had no effect on  $A\beta_{1-42}$  toxicity, while treatment of  $A\beta_{1-42}$  with **2–4** reduced the toxicity. Meptides **3** and **4** were most efficient, and treatment of **4** resulted in an MTT signal not different from that for nontreated control cells. Thus the efficiency of the meptides to rescue cells from  $A\beta$  mediated toxicity appears to increase with degree of  $N$ -methylation.

**Improvement of Longevity and Locomotor Activity in Transgenic  $A\beta_{1-42}$  *Drosophila melanogaster*.** Transgenic *Drosophila melanogaster* expressing human  $A\beta_{1-42}$  in the neurons of the central nervous system provide a model system for studying the consequences of  $A\beta_{1-42}$  aggregation in vivo.<sup>44–46</sup> The  $A\beta_{1-42}$  expressing flies exhibit a markedly reduced survival compared with wild-type flies.<sup>47</sup> Congo red,

a compound known to reduce the aggregation of  $A\beta_{1-42}$ , reduces toxicity in this *Drosophila* model of disease<sup>47</sup> and ligands designed to target the central  $A\beta$   $\alpha$ -helix are also effective,<sup>48</sup> but methylated peptides have previously not been investigated using this model. Hence, transgenic *Drosophila melanogaster* expressing  $A\beta_{1-42}$  in the central nervous system was employed to study the effects of **4** on  $A\beta_{1-42}$  toxicity in vivo by exposing the flies to the compound from the embryonic stage and throughout adult life. This treatment resulted in prolonged life span compared to nontreated counterparts (Figure 8a). No effect on life span was observed in *w*<sup>1118</sup> wild type *Drosophila* fed **4** (Supporting Information Figure S6), indicating that the mode of action of **4** is  $A\beta$  specific. *Drosophila* flies expressing  $A\beta_{1-42}$  show progressive loss of locomotor activity, eventually resulting in almost complete immobility.<sup>47</sup> A clear improvement in mobility was observed in the  $A\beta_{1-42}$  expressing flies that were fed **4**. In a climbing assay performed on 27-day-old flies kept at 29 °C, it was observed that the nontreated flies were seated at the base of the tube, showed little movement and did not climb at all, whereas the **4** treated flies climbed to the top of the tube (Figure 8b and Supporting Information movie). Thus, **4** treatment improved the locomotor activity of the  $A\beta$  expressing flies.

## Discussion and Conclusions

We have designed a series of poly-*N*-methylated peptides, which represents a first example of a peptidomimetic based on residues 32–37 of the C-terminal sequence of  $A\beta$ . One of these peptides, i.e. **4**, inhibits or slows down  $\beta$ -sheet aggregation and fibril formation, reduces toxicity of  $A\beta_{1-42}$  in vitro, and has protective effects on locomotor activity and longevity of a transgenic  $A\beta_{1-42}$  *Drosophila* flies.

Various concentration ratios (in mol) of  $A\beta$  peptide: inhibitor typically ranging from 1:1 to 1:20 have been used previously by others. Grape seed derived polyphenols were shown to be potent in inhibiting  $A\beta_{1-42}$  oligomerization at a ratio of 2:5 as determined in both cell-based and cell-free in vitro assays.<sup>30</sup> For small peptide based inhibitors, a high degree of viability and less apoptosis in PC12 cells under  $A\beta$  insult were observed when the inhibitor was used at 40-fold excess, although its inhibitory activity was shown from a molar ratio of 1:1.<sup>49</sup> D-Amino acid based peptide-inhibitors designed from the sequence 16–20 of  $A\beta$  rescued human neuroblastoma cells from  $A\beta_{1-40}$  toxicity at an optimum inhibitor concentration of 1:4.<sup>50</sup> *N*-Methylated peptides derived from sequence 16–20 also showed to be effective in the similar concentration range. These peptides showed their potential at 2–10 fold excess with respect to  $A\beta_{1-40}$  in various in vitro assays.<sup>12,14</sup> In the present study, initial TEM experiments at concentrations ranging from 1:1 to 1:10 indicated that 1:5 ratio best distinguished between the most efficient (**4**) and the less efficient (**1–3**) inhibitors, and this ratio was therefore used in further experiments.

Previously reported *N*-methylated peptides based on residues 16–20/22 of  $A\beta$  were found to bind to free peptide monomers, effectively sequestering the pool of available monomers for fibril growth.<sup>51,52</sup> In this regard, *N*-methylated amino acids placed in alternating positions had been found to be most efficient in inhibiting  $\beta$ -sheet extension during fibril formation.<sup>13</sup> Similarly,  $\beta$ -sheet breakers corresponding to the region 25–35 with either *N*-methylated Gly(33) or *N*-methylated Leu(34) prevented fibrillation or altered the fibril's

morphology in  $A\beta_{25-35}$ .<sup>53</sup> The present investigation, on the other hand, shows that a polymethylated peptide **4** is more efficient than peptides with alternating *N*-methyl groups, suggesting another mechanism of action. We believe that the rigidity conferred by poly-*N*-methylation would result in smaller loss of conformational entropy and consequently more favorable free energy upon interaction with a homologous sequence of  $A\beta$  during early self-assembly. Peptide **4** may thus interfere more with the early process of self-aggregation of  $A\beta$  by coassembling with  $A\beta$  monomers during incipient formation of oligomeric paranucleus, in a similar manner as hypothesized for nonmethylated peptide inhibitors derived from  $A\beta$  C-terminal region.<sup>17</sup> On the basis of these results, we conclude that small molecule peptidomimetics based on the C-terminal region of  $A\beta$  deserve further attention as leads for  $A\beta$  self-assembly inhibitors.

## Experimental Procedures

**Synthesis of Fmoc-*N*-methyl Amino Acids and General Procedures.** All 9-fluorenylmethoxycarbonyl (Fmoc)-protected *N*-methyl amino acids were synthesized as described.<sup>18,26</sup> High pressure liquid chromatography (HPLC) coupled to MS and universal evaporative light-scattering detection (ELSD) was done for all the synthetic compounds on a Gilson system consisting of a 322 pump, a 233 XL autosampler, and a UV/vis 152 detector, coupled in series with a Finnigan AQA mass spectrometer (electrospray in the positive mode) and an ELSD (Sedex 85 CC) from Sedere. The reverse phase HPLC analyses were done using a Phenomenex Gemini C18 (3  $\mu$ m, 3.0 mm  $\times$  150 mm) column (for purity determination) with acetonitrile–water (both containing 0.1% formic acid) as mobile phase (gradient: 5–95% acetonitrile in 6 min + 6 min at 95%, flow 1.0 mL/min). Preparative HPLC was done using a Grace Vydac C18 (5  $\mu$ m, 22 mm  $\times$  150 mm) column with acetonitrile–water (both containing 0.1% TFA) as mobile phase (gradient: 10–60% acetonitrile in 10 min + 6 min at 95%, flow 18.0 mL/min). All of the compounds were obtained in highly pure form (>95%). The HPLC retention time and corresponding ESI-MS of **1–4** have been tabulated in Supporting Information Table 1.

**Synthetic Procedures for **4**.** The peptide was synthesized according to general procedure 1A–1F described below. The amino acids Fmoc-(NMe)Val-OH, Fmoc-(NMe)Ile-OH, Fmoc-Met-OH, and Fmoc-(NMe)Gly-OH (near the N-terminal of the peptide) were coupled by method 1C. The first amino acid bound to resin, i.e. Fmoc-(NMe)Gly-OH and Fmoc-(NMe)Leu-OH, were coupled by method 1B. Each amino acid coupling was followed by deprotection of Fmoc group and washing as described under 1D.

**1A. Preparation/Deprotection of Resin.** Sieber resin (0.63 mmol/g) 0.3 g was swelled in DMF for 20 min in a reaction vessel equipped with a sintered glass bottom. A solution of 20% piperidine in DMF was then added for 10 min and then the same step was repeated for another 20 min with fresh piperidine solution. The resin was washed with 5 $\times$  DMF, 5 $\times$  MeOH, 5 $\times$  DCM, and 2 $\times$  DMF (4 mL).

**1B. Coupling of Fmoc-AA-OH or Fmoc-NMe-AA-OH to Primary Amine.** Fmoc-AA-OH or Fmoc-NMe-AA-OH (3 equiv), HATU (*O*-(7-azabenzotriazole-1-yl)-*N,N,N',N'*-tetramethyluronium hexafluorophosphate) (2.9 equiv) was dissolved in 4 mL of DMF until a clear solution was obtained. DIPEA (6 equiv) was then added and the mixture was added to the resin and stirred with the aid of nitrogen gas until a negative TNBS (2,4,6-trinitrobenzenesulfonic acid) test was obtained.

**1C. Coupling of Fmoc-AA-OH or Fmoc-NMe-AA-OH to Secondary Amine.** Fmoc-AA-OH or Fmoc-NMe-AA-OH (3 equiv), BTC (bis(trichloromethyl)carbonate) (1 equiv) was dissolved in 3 mL of THF (tetrahydrofuran) until a clear solution was obtained. 2.4.6-Collidine (8 equiv) was then added to the

solution, and a white precipitate formed in solution. Before adding the solution to the resin, the resin was pretreated with THF:DIPEA (0.6 + 0.6 mL) for 3 min. The solution was then added to the resin and stirred with the aid of nitrogen gas until a negative chloranil test was obtained. In those cases, a negative chloranil test was not obtained after 12 h, and an additional round of washing and coupling was performed as described under 1A and 1B.

**1D. Fmoc Deprotection.** The resin was washed with 5× DMF, 5× MeOH, 5× DCM, and 2× DMF (4 mL). A solution of 20% piperidine was then added for 10 min, and then the same step was repeated for another 20 min with fresh piperidine solution. An extra treatment with 2 × 5 mL DBU (1,8-diazabicyclo-[5.4.0]undec-7-ene):piperidine:toluene:DMF (5:5:20:70) for 5 min was included when secondary amines were deprotected. The resin was washed with 5× DMF, 5× MeOH, 5× DCM, and 2× DMF (4 mL) before the next coupling.

**1E. Capping of N-Terminal Amino Acid.** A solution of acetic anhydride 50 equiv (0.89 mL, 9.45 mmol) and DIPEA 50 equiv (1.65 mL, 9.45 mmol) was dissolved in 3 mL of DMF and added to the washed resin. After 40 min, the resin was washed with 5× DMF, 5× MeOH, and 5× DCM (4 mL).

**1F. Cleavage of Peptide from Resin.** The resin was washed with 10× DCM (4 mL) before cleavage to wash away residual DMF. The peptide was cleaved from the resin using DCM:TFA:EDT (1,2-ethanedithiol) (97.9:2:0.1) (5 mL) for 15 min. The cleavage solution was collected into a flask containing 25 mL of toluene. Then the resin was washed with 5× DCM, 5× MeOH, 5× DCM, and 5× MeOH (4 mL) to wash out residual cleaved peptide. The cleavage solution was then evaporated and gave a slightly yellow oil. A white solid precipitated upon addition of water to the yellow oil, the mixture was sonicated, and acetonitrile was added until a clear solution was obtained. The solution was then lyophilized. The obtained white material was purified using preparative HPLC.

The synthetic procedures for peptides **1**, **2**, and **3** have been described in the Supporting Information.

**Preparation of  $A\beta_{1-40}$  and  $A\beta_{1-42}$ .**  $A\beta_{1-40}$  or  $A\beta_{1-42}$  (1 mg) was dissolved in 1 mL of trifluoroacetic acid (TFA), and the TFA was removed under a gentle stream of argon. The peptide was then suspended in 1 mL of 1,1,1,3,3,3-hexafluoro-2-propanol (HFIP) and incubated at 37 °C for 1 h. The HFIP was evaporated under a stream of argon, and the resulting peptide film was dissolved in 2 mL HFIP and aliquoted. HFIP was evaporated under argon, and the vials were kept for 3 h under 0.5 mbar to remove traces of HFIP. The aliquots were stored in an airtight vial at -20 °C. Immediately prior to use, the aliquots were dissolved to 200  $\mu$ M in 20 mM NaOH followed by brief sonication (15 s). This solution was diluted to 20 or 25  $\mu$ M in 10 mM sodium phosphate buffer, pH 7.4, for all experiments.

**TEM.**  $A\beta_{1-40}$  (25  $\mu$ M) was mixed with 125  $\mu$ M **1–4** in 10 mM sodium phosphate buffer, pH 7. At specified time points, aliquots of 2  $\mu$ L of  $A\beta$ -inhibitor samples were adsorbed for 1 min on 200-mesh copper grids and stained with 2% uranylacetate for 30 s before being examined and photographed using a Hitachi H7100 microscope operated at 75 or 100 kV.

**AFM.** At specific time points, aliquots of 2  $\mu$ L of the incubated  $A\beta$ -inhibitor samples were dropped on freshly cleaved mica surface and left for 2 min. Then the mica plate containing the drop of sample solution was washed gently with drops of deionized water and subsequently dried under dry argon. All the AFM measurements were performed in tapping mode using a Nanoscope 3a multimode instrument from VEECO.

**CD Spectroscopy.**  $A\beta_{1-40}$  or  $A\beta_{1-42}$  (20  $\mu$ M) were mixed with 100  $\mu$ M **1–4** in 10 mM sodium phosphate buffer, pH 7. CD spectra were obtained using a Jasco-810-150S spectropolarimeter (Jasco, Japan). A quartz cell with 1 mm optical path was used. Spectra were recorded at 25 °C between 190 and 260 nm with a bandwidth of 1 nm, a 2 s response time, and a scan speed

of 50 nm/min. Background spectra and when applicable, spectra of **1–4**, were subtracted. Each spectrum represents the average of three consecutive scans. Deconvolution of CD spectra have been performed using SELCON3 program.<sup>35,36</sup>

**Congo Red Binding.**  $A\beta_{1-40}$  or  $A\beta_{1-42}$  (20  $\mu$ M solution in 10  $\mu$ M sodium phosphate buffer, pH 7.4) was incubated in the presence and absence of 100  $\mu$ M of **1–4** at 37 °C under agitation. At different time points, 100  $\mu$ L of each sample was added to 66.6  $\mu$ L of 100  $\mu$ M stock solution of Congo red in 90% filtered phosphate buffered saline (PBS) and 10% v/v ethanol and left at 22 °C for 15 min after brief vortexing. Readings were taken on a Cary 300 Bio UV–visible spectrophotometer at 403 and 541 nm with a blank of Congo red. Contributions from **1–4** were subtracted and the amount of Congo red bound was calculated as described.<sup>38</sup> Data from three independent experiments were combined to statistically validate the results.

**Cell Experiments.** Rat pheochromocytoma cells (PC12 cells) were cultured in 5% carbon dioxide in DMEM medium supplemented with 10% fetal calf serum, 10% horse serum, and penicillin/streptomycin (National Veterinary Institute, Sweden). The cells were plated in 96-well Cell+ plates (Sarstedt, Sweden). The following day, the media was exchanged to DMEM without phenol red (90  $\mu$ L/well) supplemented with 10% fetal calf serum and penicillin/streptomycin.  $A\beta_{1-42}$  at 20  $\mu$ M was added (10  $\mu$ L/well), resulting in a final concentration of 2  $\mu$ M with or without **1–4** at five times molar excess. PBS was used as control treatment. The cells were incubated for 4 h and thereafter MTT (3-(4, 5-dimethylthiazol-2-yl)-2-5 diphenyltetrazolium bromide) dissolved at 1 mg/mL in DMEM without phenol red was added (50  $\mu$ L/well) and incubated with the cells for 2 h at 37 °C. The purple formazan crystals were dissolved using 50% dimethylformamide and 20% SDS in water added directly to the cell culture media (100  $\mu$ L/well), and absorbance at 575 nm was recorded.

**Experiments with Flies.**  $A\beta_{1-42}$  transgenic *Drosophila melanogaster* strains were generated as described in Crowther et al.<sup>47</sup> Transgenic flies expressing one gene copy of human  $A\beta_{1-42}$  were obtained by crossing  $A\beta$  flies with flies transgenic for the Gal4-*elav*<sup>el155</sup> pan-neuronal driver. Flies expressing  $A\beta_{1-42}$  were incubated in groups of 10 in 10 cm glass vials. Wild type  $w^{1118}$  flies treated the same way as the  $A\beta$  flies were used as controls. The flies were kept at 29 °C and high humidity. Larvae were fed instant fly food containing 300  $\mu$ M **4** until eclosion. Thereafter, flies were fed standard fly food with a streak of yeast paste containing the same amount as stated above of **4**. Food was changed every second day and viable flies were counted. Survival data were analyzed using the WinStat Kaplan–Maier software package (R. Fitch Software, Germany). Longevity of the flies depends substantially on conditions such as humidity and temperature and therefore varies between experimental occasions. For that reason, treated and nontreated control  $A\beta_{1-42}$ -expressing flies and  $w^{1118}$  wild type flies were kept under identical conditions.

**Acknowledgment.** We are grateful to Dr. Damian Crowther for gift of flies. This work was supported by a grant from Stiftelsen Olle Engkvist Byggnästare and by the Swedish Research Council. The Wenner-Gren Foundation and the Swedish Brain Foundation are gratefully acknowledged for post doctoral fellowships to T.G. and A.S., respectively.

**Note Added after ASAP Publication.** This paper was published ASAP on November 5, 2009 with an incorrect video file for Supporting Information. The revised version was published on November 13, 2009.

**Supporting Information Available:** CD of inhibitors and residual molar ellipticity at 217 nm, structures of (N-Me-Ala)<sub>5</sub> and **40x**, TEM, data of  $A\beta$  fibrils by AFM, survival of control

flies, table of fibril abundance and appearance by TEM, video (AVI) of locomotor activity of treated vs nontreated flies, and details of synthesis. This material is available free of charge via the Internet at <http://pubs.acs.org>.

## References

- Roychaudhuri, R.; Yang, M.; Hoshi, M. M.; Teplow, D. B. Amyloid  $\beta$ -Protein Assembly and Alzheimer Disease. *J. Biol. Chem.* **2009**, *284*, 4749–4753.
- Petkova, A. T.; Leapman, R. D.; Guo, Z.; Yau, W. M.; Mattson, M. P.; Tycko, R. Self-propagating, molecular-level polymorphism in Alzheimer's  $\beta$ -amyloid fibrils. *Science* **2005**, *307*, 262–265.
- Pimplikar, S. W. Reassessing the amyloid cascade hypothesis of Alzheimer's disease. *Int. J. Biochem. Cell Biol.* **2009**, *41*, 1261–1268.
- Barghorn, S.; Nimmrich, V.; Striebinger, A.; Krantz, C.; Keller, P.; Janson, B.; Bahr, M.; Schmidt, M.; Bitner, R. S.; Harlan, J.; Barlow, E.; Ebert, U.; Hillen, H. Globular amyloid  $\beta$ -peptide oligomer—a homogenous and stable neuropathological protein in Alzheimer's disease. *J. Neurochem.* **2005**, *95*, 834–847.
- Viola, K. L.; Velasco, P. T.; Klein, W. L. Why Alzheimer's is a disease of memory: the attack on synapses by  $A\beta$  oligomers (ADDLs). *J. Nutr., Health Aging* **2008**, *12*, 51S–57S.
- Ferreira, S. T.; Vieira, M. N.; De Felice, F. G. Soluble protein oligomers as emerging toxins in Alzheimer's and other amyloid diseases. *IUBMB Life* **2007**, *59*, 332–345.
- Martins, I. C.; Kuperstein, I.; Wilkinson, H.; Maes, E.; Vanbrabant, M.; Jonckheere, W.; Van Gelder, P.; Hartmann, D.; D'Hooge, R.; De Strooper, B.; Schymkowitz, J.; Rousseau, F. Lipids revert inert  $A\beta$  amyloid fibrils to neurotoxic protofibrils that affect learning in mice. *EMBO J.* **2008**, *27*, 224–233.
- Findeis, M. A. Approaches to discovery and characterization of inhibitors of amyloid  $\beta$ -peptide polymerization. *Biochim. Biophys. Acta* **2000**, *1502*, 76–84.
- Goldsbury, C. S.; Wirtz, S.; Muller, S. A.; Sunderji, S.; Wicki, P.; Aebi, U.; Frey, P. Studies on the in vitro assembly of  $A\beta$  1–40: implications for the search for  $A\beta$  fibril formation inhibitors. *J. Struct. Biol.* **2000**, *130*, 217–231.
- Nerelius, C.; Johansson, J.; Sandegren, A. Amyloid  $\beta$ -peptide aggregation. What does it result in and how can it be prevented? *Front. Biosci.* **2009**, *14*, 1716–1729.
- Adessi, C.; Frossard, M. J.; Boissard, C.; Fraga, S.; Bieler, S.; Ruckle, T.; Vilbois, F.; Robinson, S. M.; Mutter, M.; Banks, W. A.; Soto, C. Pharmacological profiles of peptide drug candidates for the treatment of Alzheimer's disease. *J. Biol. Chem.* **2003**, *278*, 13905–13911.
- Gordon, D. J.; Tappe, R.; Meredith, S. C. Design and characterization of a membrane permeable *N*-methyl amino acid-containing peptide that inhibits  $A\beta$ 1–40 fibrillogenesis. *J. Pept. Res.* **2002**, *60*, 37–55.
- Gordon, D. J.; Sciarretta, K. L.; Meredith, S. C. Inhibition of  $\beta$ -amyloid(40) fibrillogenesis and disassembly of  $\beta$ -amyloid(40) fibrils by short  $\beta$ -amyloid congeners containing *N*-methyl amino acids at alternate residues. *Biochemistry* **2001**, *40*, 8237–8245.
- Cruz, M.; Tusell, J. M.; Grillo-Bosch, D.; Albericio, F.; Serratos, J.; Rabanal, F.; Giralt, E. Inhibition of  $\beta$ -amyloid toxicity by short peptides containing *N*-methyl amino acids. *J. Pept. Res.* **2004**, *63*, 324–328.
- Kokkoni, N.; Stott, K.; Amijee, H.; Mason, J. M.; Doig, A. J. *N*-Methylated peptide inhibitors of  $\beta$ -amyloid aggregation and toxicity. Optimization of the inhibitor structure. *Biochemistry* **2006**, *45*, 9906–9918.
- Jarrett, J. T.; Berger, E. P.; Lansbury, P. T., Jr. The carboxy terminus of the  $\beta$  amyloid protein is critical for the seeding of amyloid formation: implications for the pathogenesis of Alzheimer's disease. *Biochemistry* **1993**, *32*, 4693–4697.
- Fradinger, E. A.; Monien, B. H.; Urbanc, B.; Lomakin, A.; Tan, M.; Li, H.; Spring, S. M.; Condrón, M. M.; Cruz, L.; Xie, C. W.; Benedek, G. B.; Bitan, G. C-Terminal peptides coassemble into  $A\beta$ 42 oligomers and protect neurons against  $A\beta$ 42-induced neurotoxicity. *Proc. Natl. Acad. Sci. U.S.A.* **2008**, *105*, 14175–14180.
- Zhang, S.; Prabpai, S.; Kongsaree, P.; Arvidsson, P. I. Poly-*N*-methylated alpha-peptides: synthesis and X-ray structure determination of  $\beta$ -strand forming foldamers. *Chem. Commun.* **2006**, 497–499.
- Bitan, G.; Kirkitadze, M. D.; Lomakin, A.; Vollers, S. S.; Benedek, G. B.; Teplow, D. B. Amyloid  $\beta$ -protein ( $A\beta$ ) assembly:  $A\beta$  40 and  $A\beta$  42 oligomerize through distinct pathways. *Proc. Natl. Acad. Sci. U.S.A.* **2003**, *100*, 330–335.
- Dahlgren, K. N.; Manelli, A. M.; Stine, W. B., Jr.; Baker, L. K.; Krafft, G. A.; LaDu, M. J. Oligomeric and fibrillar species of amyloid- $\beta$  peptides differentially affect neuronal viability. *J. Biol. Chem.* **2002**, *277*, 32046–32053.
- Urbanc, B.; Cruz, L.; Yun, S.; Buldyrev, S. V.; Bitan, G.; Teplow, D. B.; Stanley, H. E. In silico study of amyloid  $\beta$ -protein folding and oligomerization. *Proc. Natl. Acad. Sci. U.S.A.* **2004**, *101*, 17345–17350.
- Yun, S.; Urbanc, B.; Cruz, L.; Bitan, G.; Teplow, D. B.; Stanley, H. E. Role of electrostatic interactions in amyloid  $\beta$ -protein ( $A\beta$ ) oligomer formation: a discrete molecular dynamics study. *Biophys. J.* **2007**, *92*, 4064–4077.
- Bitan, G.; Tarus, B.; Vollers, S. S.; Lashuel, H. A.; Condrón, M. M.; Straub, J. E.; Teplow, D. B. A molecular switch in amyloid assembly: Met35 and amyloid  $\beta$ -protein oligomerization. *J. Am. Chem. Soc.* **2003**, *125*, 15359–15365.
- Teixido, M.; Belda, I.; Zurita, E.; Llorca, X.; Fabre, M.; Vilaro, S.; Albericio, F.; Giralt, E. Evolutionary combinatorial chemistry, a novel tool for SAR studies on peptide transport across the blood–brain barrier. Part 2. Design, synthesis and evaluation of a first generation of peptides. *J. Pept. Sci.* **2005**, *11*, 789–804.
- Biron, E.; Chatterjee, J.; Kessler, H. Optimized selective *N*-methylation of peptides on solid support. *J. Pept. Sci.* **2006**, *12*, 213–219.
- Govender, T.; Arvidsson, P. I. Facile synthesis of Fmoc-*N*-methylated  $\alpha$ - and  $\beta$ -amino acids. *Tetrahedron Lett.* **2006**, *47*, 1691–1694.
- Bartolini, M.; Bertucci, C.; Bolognesi, M. L.; Cavalli, A.; Melchiorre, C.; Andrisano, V. Insight into the kinetic of amyloid  $\beta$  (1–42) peptide self-aggregation: elucidation of inhibitors' mechanism of action. *ChemBioChem* **2007**, *8*, 2152–2161.
- Teplow, D. B. Preparation of amyloid  $\beta$ -protein for structural and functional studies. *Methods Enzymol.* **2006**, *413*, 20–33.
- Goldbeck, R. A.; Thomas, Y. G.; Chen, E.; Esquerra, R. M.; Kliger, D. S. Multiple pathways on a protein-folding energy landscape: kinetic evidence. *Proc. Natl. Acad. Sci. U.S.A.* **1999**, *96*, 2782–2787.
- Ono, K.; Condrón, M. M.; Ho, L.; Wang, J.; Zhao, W.; Pasinetti, G. M.; Teplow, D. B. Effects of grape seed-derived polyphenols on amyloid  $\beta$ -protein self-assembly and cytotoxicity. *J. Biol. Chem.* **2008**, *283*, 32176–32187.
- Kirkitadze, M. D.; Condrón, M. M.; Teplow, D. B. Identification and characterization of key kinetic intermediates in amyloid  $\beta$ -protein fibrillogenesis. *J. Mol. Biol.* **2001**, *312*, 1103–1119.
- Murakami, K.; Irie, K.; Ohigashi, H.; Hara, H.; Nagao, M.; Shimizu, T.; Shirasawa, T. Formation and stabilization model of the 42-mer  $A\beta$  radical: implications for the long-lasting oxidative stress in Alzheimer's disease. *J. Am. Chem. Soc.* **2005**, *127*, 15168–15174.
- Riek, R.; Guntert, P.; Dobeli, H.; Wipf, B.; Wuthrich, K. NMR studies in aqueous solution fail to identify significant conformational differences between the monomeric forms of two Alzheimer peptides with widely different plaque-competence,  $A\beta$ (1–40)(ox) and  $A\beta$ (1–42)(ox). *Eur. J. Biochem.* **2001**, *268*, 5930–5936.
- Sgourakis, N. G.; Yan, Y.; McCallum, S. A.; Wang, C.; Garcia, A. E. The Alzheimer's peptides  $A\beta$ 40 and 42 adopt distinct conformations in water: a combined MD/NMR study. *J. Mol. Biol.* **2007**, *368*, 1448–1457.
- Sreerama, N.; Woody, R. W. A self-consistent method for the analysis of protein secondary structure from circular dichroism. *Anal. Biochem.* **1993**, *209*, 32–44.
- Whitmore, L.; Wallace, B. A. Protein secondary structure analyses from circular dichroism spectroscopy: methods and reference databases. *Biopolymers* **2008**, *89*, 392–400.
- Ono, K.; Condrón, M. M.; Teplow, D. B. Structure–neurotoxicity relationships of amyloid  $\beta$ -protein oligomers. *Proc. Natl. Acad. Sci. U.S.A.* **2009**, DOI: 10.1073/pnas.0905127106
- Klunk, W. E.; Pettegrew, J. W.; Abraham, D. J. Quantitative evaluation of congo red binding to amyloid-like proteins with a  $\beta$ -pleated sheet conformation. *J. Histochem. Cytochem.* **1989**, *37*, 1273–1281.
- Costa, R.; Goncalves, A.; Saraiva, M. J.; Cardoso, I. Transthyretin binding to  $A\beta$  peptide – impact on  $A\beta$  fibrillogenesis and toxicity. *FEBS Lett.* **2008**, *582*, 936–942.
- Arimon, M.; Diez-Perez, I.; Kogan, M. J.; Durany, N.; Giralt, E.; Sanz, F.; Fernandez-Busquets, X. Fine structure study of  $A\beta$ 1–42 fibrillogenesis with atomic force microscopy. *FASEB J.* **2005**, *19*, 1344–1346.
- Mastrangelo, I. A.; Ahmed, M.; Sato, T.; Liu, W.; Wang, C.; Hough, P.; Smith, S. O. High-resolution atomic force microscopy of soluble  $A\beta$ 42 oligomers. *J. Mol. Biol.* **2006**, *358*, 106–119.
- Liu, Y.; Schubert, D. Cytotoxic amyloid peptides inhibit cellular 3-(4,5-dimethylthiazol-2-yl)-2,5-diphenyltetrazolium bromide (MTT) reduction by enhancing MTT formazan exocytosis. *J. Neurochem.* **1997**, *69*, 2285–2293.

- (43) Liu, Y.; Peterson, D. A.; Kimura, H.; Schubert, D. Mechanism of cellular 3-(4,5-dimethylthiazol-2-yl)-2,5-diphenyltetrazolium bromide (MTT) reduction. *J. Neurochem.* **1997**, *69*, 581–593.
- (44) Rival, T.; Page, R. M.; Chandraratna, D. S.; Sendall, T. J.; Ryder, E.; Liu, B.; Lewis, H.; Rosahl, T.; Hider, R.; Camargo, L. M.; Shearman, M. S.; Crowther, D. C.; Lomas, D. A. Fenton chemistry and oxidative stress mediate the toxicity of the  $\beta$ -amyloid peptide in a *Drosophila* model of Alzheimer's disease. *Eur. J. Neurosci.* **2009**, *29*, 1335–1347.
- (45) Crowther, D. C.; Page, R.; Chandraratna, D.; Lomas, D. A. A *Drosophila* model of Alzheimer's disease. *Methods Enzymol.* **2006**, *412*, 234–255.
- (46) Luheshi, L. M.; Tartaglia, G. G.; Brorsson, A. C.; Pawar, A. P.; Watson, I. E.; Chiti, F.; Vendruscolo, M.; Lomas, D. A.; Dobson, C. M.; Crowther, D. C. Systematic in vivo analysis of the intrinsic determinants of amyloid  $\beta$  pathogenicity. *PLoS Biol.* **2007**, *5*, e290.
- (47) Crowther, D. C.; Kinghorn, K. J.; Miranda, E.; Page, R.; Curry, J. A.; Duthie, F. A.; Gubb, D. C.; Lomas, D. A. Intraneuronal A $\beta$ , non-amyloid aggregates and neurodegeneration in a *Drosophila* model of Alzheimer's disease. *Neuroscience* **2005**, *132*, 123–135.
- (48) Nerelius, C.; Sandegren, A.; Sargsyan, H.; Raunak, R.; Leijonmarck, H.; Chatterjee, U.; Fisahn, A.; Imarisio, S.; Lomas, D. A.; Crowther, D. C.; Stromberg, R.; Johansson, J. Alpha-helix targeting reduces amyloid- $\beta$  peptide toxicity. *Proc. Natl. Acad. Sci. U.S.A.* **2009**, *106*, 9191–9196.
- (49) Frydman-Marom, A.; Rechter, M.; Shefler, I.; Bram, Y.; Shalev, D. E.; Gazit, E. Cognitive-Performance Recovery of Alzheimer's Disease Model Mice by Modulation of Early Soluble Amyloid Assemblies. *Angew. Chem., Int. Ed.* **2008**, *48*, 1981–1986.
- (50) Chalifour, R. J.; McLaughlin, R. W.; Lavoie, L.; Morissette, C.; Tremblay, N.; Boule, M.; Sarazin, P.; Stea, D.; Lacombe, D.; Tremblay, P.; Gervais, F. Stereoselective interactions of peptide inhibitors with the  $\beta$ -amyloid peptide. *J. Biol. Chem.* **2003**, *278*, 34874–34881.
- (51) Soto, P.; Griffin, M. A.; Shea, J. E. New insights into the mechanism of Alzheimer amyloid- $\beta$  fibrillogenesis inhibition by *N*-methylated peptides. *Biophys. J.* **2007**, *93*, 3015–3025.
- (52) Chebaro, Y.; Derreumaux, P. Targeting the early steps of A $\beta$ 16–22 protofibril disassembly by *N*-methylated inhibitors: a numerical study. *Proteins* **2009**, *75*, 442–452.
- (53) Hughes, E.; Burke, R. M.; Doig, A. J. Inhibition of toxicity in the  $\beta$ -amyloid peptide fragment  $\beta$ -(25–35) using *N*-methylated derivatives: a general strategy to prevent amyloid formation. *J. Biol. Chem.* **2000**, *275*, 25109–25115.